Presence and origin of interface charges at atomic-layer deposited Al_2O_3/III-nitride heterojunctions

Satyaki Ganguly, Jai Verma, Guowang Li, Tom Zimmermann, Huili Xing, and Debdeep Jena[a)]
Department of Electrical Engineering, University of Notre Dame, Notre Dame, Indiana 46556, USA

(Received 13 June 2011; accepted 14 October 2011; published online 9 November 2011)

Unlike silicon and traditional III-V semiconductors, the III-nitrides exhibit high spontaneous and piezoelectric polarization charges at epitaxial polar heterojunctions. In the process of investigating scaling properties of gate-stacks consisting atomic-layer deposited Al_2O_3/III-Nitride heterojunctions, we find interface charges that appear closely linked to the polarization charges of the underlying nitride substrate. Through capacitance-voltage measurement on a series of samples of varying dielectric thicknesses, we find the presence and propose an origin of benign donor-type interface charges (Q_{it} $\sim 6 \times 10^{13}$ cm^{-2}) at the AlN/Al_2O_3 junction. This interface charge is almost equal to the net polarization charge in AlN. The polarization-related dielectric/AlN interface charge and the role of oxygen in the dielectric as a possible modulation dopant potentially offer opportunities for various device applications. © *2011 American Institute of Physics*. [doi:10.1063/1.3658450]

GaN high electron mobility transistors (HEMTs) outperform Si devices for high voltage switching by virtue of their large bandgap and additionally possess the potential for very high speed switching. This requires highly scaled low sheet-resistance HEMT structures with very thin barriers. However, ultrathin epitaxial barriers (such as AlN or InAlN) result in substantial leakage currents preventing the capability to block high drain voltages, and dielectrics can substantially mitigate this problem. Thus, dielectrics such as SiO_2,[1] Si_3N_4,[2] HfO_2,[3] and Al_2O_3 (Ref. 4) are being investigated intensively both for composite gate stacks as well as for the suppression of current collapse[5] by passivating surface states in these devices. Atomic layer deposited (ALD) Al_2O_3 has drawn the attention of the community due to its large bandgap and outstanding dielectric[6] and passivation[7] properties. The superior quality (in terms of uniformity) of ALD over sputtering and electron-beam deposition, coupled with high band gap ($\sim$6.5 eV),[8] high dielectric constant ($\sim$9.1), high break down field ($\sim$10MV/cm), high thermal (amorphous $\sim$1000 °C), and chemical stability of ALD-grown Al_2O_3 makes it a natural choice as a gate insulator for AlN/GaN HEMTs (Ref. 9) and its variants. The study of the ALD Al_2O_3/III-nitride interface is of prime importance for device characteristics of AlN/GaN HEMTs. In this work, we present a comprehensive characterization of AlN/GaN MOS-HEMT gate stacks with ALD Al_2O_3 of various thicknesses. Through capacitance-voltage (C-V) measurement, we find the presence and propose an origin of benign donor-type positive interface charge (Q_{it}) at the AlN/Al_2O_3 junction and relate its presence to the polarization charges in AlN. The presence of Q_{it} explains the trend of pinch-off voltage and two-dimensional electron gas (2DEG) density with ALD thicknesses both qualitatively and quantitatively. Recent report[10] (appeared after this submission) on ALD/GaN structure also invokes positive interface charge to explain the trend of pinch-off voltage with ALD thicknesses.

AlN/GaN HEMT structures were grown in a Veeco Gen 930 molecular beam epitaxy (MBE) system on semi insulating 0001 GaN templates (2 μm) on sapphire under metal rich conditions. Ga flux of $\sim 2.1 \times 10^{-7}$ Torr, Al flux of $\sim 1.6 \times 10^{-7}$ Torr, and N_2 supplied from a Veeco rf source at a plasma power of 240 W were used. The MBE layer structure consisted of a thin 1.5 nm AlN nucleation layer (to eliminate buffer leakage[11]), followed by 240 nm unintentionally doped (UID) GaN, and $t_{AlN} = 4$ nm AlN barrier layer grown at a substrate thermocouple temperature of 660 °C as indicated in Fig 1(a). Mesa isolation was achieved with BCl_3/Cl_2 plasma reactive ion etching, followed by source/drain ohmic metallization using Ti/Al/Ni/Au (15/120/40/60 nm) stack deposition followed by rapid thermal annealing in N_2/Ar atmosphere for 30 s at 600 °C. A saturation current of 1.3 Amps/mm was measured. The sample was then cleaved into four parts and four different Al_2O_3 thicknesses ($t_{ox} = 2$ nm, 4 nm, 6 nm, and 8 nm) were deposited on the AlN surface by ALD with tri methyl aluminum (TMA) and H_2O as the precursors under identical conditions at 200 °C. Finally, Ni/Au

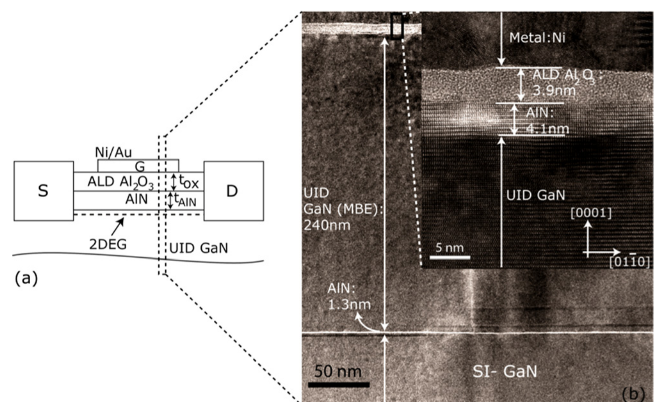

FIG. 1. (Color online) (a) Schematic layer structure of the sample; (b) high resolution transmission electron microscope image along zone axis [100] showing the layer structure of the sample; High-resolution lattice image of the gate stack (inset) showing the crystalline AlN barrier layer, the amorphous ALD Al_2O_3, and Ni as gate metal.

a)Author to whom correspondence should be addressed. Electronic mail: Debdeep.Jena.1@nd.edu.

 © 2011 American Institute of Physics

Downloaded 09 Nov 2011 to 129.74.250.206. Redistribution subject to AIP license or copyright; see http://apl.aip.org/about/rights_and_permissions

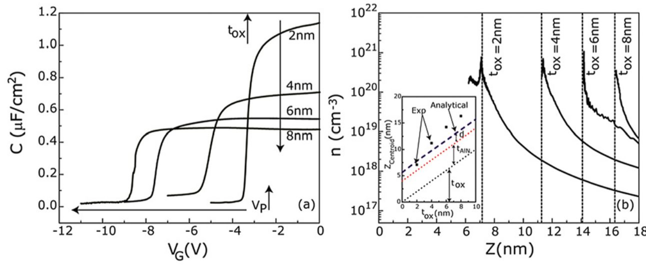

FIG. 2. (Color online) (a) C-V plots (@1 MHz) of the four samples with different t_{ox} showing V_p increases with increasing t_{ox}; (b) Plots showing the charge profile and varying depth of 2DEG channel from the gate metal for samples with different t_{ox}. Experimentally and analytically obtained 2DEG peak position for different t_{ox} is shown in the inset (b).

(50/150 nm) gate metal stacks were deposited simultaneously on the 4 samples. The layer structure of the sample is shown in Fig. 1(a). Fig. 1(b) shows the cross-section transmission electron microscopy (TEM) image of the gate stack of the $t_{ox} = 4$ nm sample, confirming the thicknesses. The thickness variation of the ALD Al_2O_3 layer is within an acceptable window. The C-V characteristics measured at 1 MHz on circular diode patterns of area $A = \pi \times (10\,\mu m)^2$ on the four samples with different t_{ox} shows negligible hysteresis. As shown in Fig. 2(a), the pinch-off voltage V_p increased with the thickness of the ALD oxide (as deposited and unannealed) layer from $V_p = -3.6$ V for $t_{ox} = 2$ nm to $V_p = -8.8$ V for $t_{ox} = 8$ nm. The carrier density profile $n(z)$ extracted[12] from the C-V measurement using $n(z) = (C^3/q\varepsilon_s)(dC/dV)^{-1}$ is shown in Fig. 2(b), indicating the varying depth of the 2DEG channel from the gate metal. The centroid of the 2DEG distribution from the ALD surface is given by $z_{centroid} = t_{ox} + t_{AlN} + d$. Where d is the displacement of the centroid of the 2DEG from the heterointerface (AlN/GaN) and is given by $d = 3/b$ ($b = 132\pi^2 m^* q^2 n_s / 8h^2 \varepsilon_s$).[13] Fig. 2(b): inset shows the comparison of the 2DEG peak position as obtained from the analytical expression above with the one obtained from the experimental result (extracted from the C-V measurement).

To explain the increase in V_p with t_{ox} for the structures, we investigate possible sources of fixed/mobile charges and associated energy band diagrams. Apart from fixed polarization charges at the epitaxial AlN/GaN heterojunction and the AlN surface, we consider a fixed positive sheet charge (Q_{it}) at the ALD/AlN interface (justified later). Fig. 3(a) shows the charge and energy band diagram simulated using a self-consistent Poisson-Schrödinger solver[14] for the Ni/Al_2O_3/AlN/GaN (50/2/4/240 nm) structure at $V_G = 0$ V with and without Al_2O_3/AlN interface oxide charges. The charge and energy band diagram at pinch-off ($V_G = V_p$) is shown in Fig. 3(b). From this figure, the generalized expression for V_p is

$$qV_p = -\phi_B + (qV^p_{AlN} + qV^p_{ox}) + (\Delta E_c^{AlN/GaN} - \Delta E_c^{ox/AlN}), \tag{1}$$

where V^p_{AlN} and V^p_{ox} are the voltage drops at pinch-off in the AlN and oxide layer, respectively, given by

$$V^p_{AlN} = qQ_{\pi(AlN/GaN)}(t_{AlN}/\varepsilon_{AlN}), \tag{2}$$

$$V^p_{ox} = q(Q_{it} - Q_{\pi(GaN)})(t_{ox}/\varepsilon_{ox}). \tag{3}$$

Here, $Q_{\pi(AlN/GaN)}$ ($\sim 6.1 \times 10^{13}\,cm^{-2}$) is the polarization charge density at the AlN/GaN interface, $Q_{\pi(GaN)}$ ($\sim 1.8 \times 10^{13}\,cm^{-2}$) the polarization charge density of GaN, t_{AlN} the thickness of AlN, t_{ox} the thickness of the ALD oxide layer, ε_{AlN} ($\sim 9.1\varepsilon_0$) is the dielectric constant of AlN and ε_{ox} ($\sim 9.1\varepsilon_0$) of the ALD oxide, $\Delta E_c{}^{AlN/GaN}$ (~ 1.9 eV) is the conduction band offset between AlN/GaN, and $\Delta E_c{}^{ox/AlN} \sim (\chi_{AlN} - \chi_{Al2O3} \sim 1.3\,eV)$[15,16] is the conduction band offset between Al_2O_3/AlN. We extract $\Phi_B = 2.9$ eV to be the Ni/Al_2O_3 surface barrier height from the slope of a Fowler-Nordheim[17] plot of a (Ni/Al_2O_3/Ni) M-I-M diode structure (not shown here). We note that at pinch-off (Fig 3(b)), the details of the energy band diagram from the bulk till the AlN/Al_2O_3 interface remain locked by the requirements of no charge in the channel and the polarization charges at the AlN/GaN interface and the AlN surface. From Eq. (1), it is evident that if the ALD layer introduces no additional charges ($Q_{it} = 0$), then V_p should tend towards zero (decrease). It may even be possible to make $V_p > 0$ this way, achieving enhancement mode (E-Mode) operation by simply

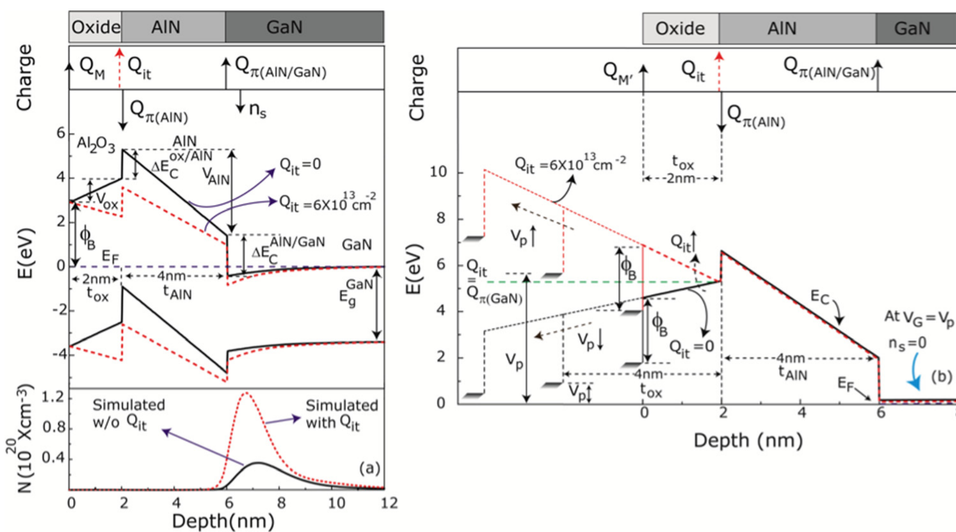

FIG. 3. (Color online) (a) Charge distribution, simulated energy band diagram, and carrier profile of Ni/Al_2O_3/AlN/GaN at $V_G = 0$ (w and w/o Q_{it}); (b) Charge distribution and simulated conduction band diagram of Ni/Al_2O_3/AlN/GaN at $V_G = V_p$ for different Q_{it}. Plots showing that for $Q_{it} = 0$, V_p decreases with increasing t_{ox}, for $Q_{it} = Q_{\pi(GaN)}$, V_p remains constant with t_{ox} and for $Q_{it} = 6 \times 10^{13}\,cm^{-2}$, V_p increases with increasing t_{ox}.

Downloaded 09 Nov 2011 to 129.74.250.206. Redistribution subject to AIP license or copyright; see http://apl.aip.org/about/rights_and_permissions

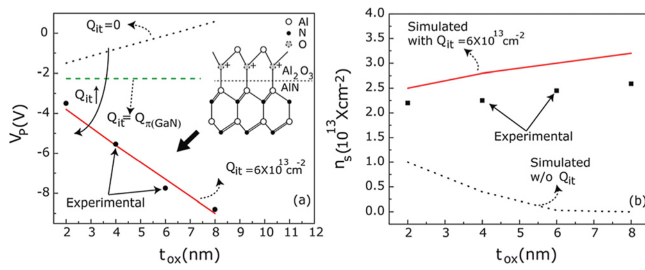

FIG. 4. (Color online) (a)-(b) Experimental and simulated (for various Q_{it}) V_p and n_s for different t_{ox}. The atomic arrangements at the Al_2O_3/AlN interface and the positive donor dopants giving rise to Q_{it} are shown in the inset (a).

growing a charge-free dielectric in the gate region. This is the consequence of polarization charges at III-nitride heterojunctions that prevent flat-band conditions through the entire structure under *any* bias voltage. However, the experimental shifts of V_p in Fig. 2(a) contradict this trend. We find that introducing a positive charge $Q_{it} \sim 6\times10^{13}\,\mathrm{cm}^{-2}$ at the (Al_2O_3/AlN) interface captures the V_p shifts as shown in Fig. 3(b). This value is essentially identical to the net polarization charge in the strained AlN layer ($Q_{it} \sim Q_{\pi(AlN/GaN)}$). On the other hand if the interface charge is equal to the net spontaneous polarization of GaN ($Q_{it} = Q_{\pi(GaN)}$), V_p should not change with t_{ox} as also shown in Fig. 3(b). Thus, with the increase of t_{ox}, if $Q_{it} < Q_{\pi(GaN)}$, V_p will decrease (become more E-mode) and if $Q_{it} > Q_{\pi(GaN)}$, V_p will increase (become more depletion mode (D-mode)).

The increase in experimental V_p with t_{ox} is *quantitatively* justified (with $Q_{it} \sim 6\times10^{13}\,\mathrm{cm}^{-2}$) by using self-consistent Poisson-Schrödinger simulation as shown in Fig. 4(a). The interface density $Q_{it} \sim 6\times10^{13}\,\mathrm{cm}^{-2}$ is remarkably close to the surface polarization charge of the strained AlN layer. We argue that since the AlN surface is metal (Al)-face, the oxygen atoms of the ALD layer attach to Al and by electron counting rules can be viewed as substituting the nitrogen site,[18] acting as donor dopants. The picture is essentially identical to modulation doping: the positive sheet charge at the Al_2O_3/AlN interface [inset, Fig. 4(a)] neutralizes negative polarization charges of the AlN surface, increasing the 2DEG density at the AlN/GaN heterojunction. Fig. 4(b) shows that the increase in the experimental 2DEG density n_s (from C-V) with t_{ox} can be explained if $Q_{it} \sim 6\times10^{13}\,\mathrm{cm}^{-2}$ is assumed.

In conclusion, we have systematically analyzed the properties of metal-polar AlN/GaN interface with ALD Al_2O_3 insulator. Our result indicates that the negative polarization charge at the AlN surface is effectively compensated by fixed positive charge ($Q_{it} \sim 6\times10^{13}\,\mathrm{cm}^{-2}$). The role of ALD oxygen layers as possible modulation dopants can offer opportunities for various innovative designs in III-nitride electronic devices. Recently, it has been demonstrated[19] that the deposition of ALD Al_2O_3/Si_3N_4 on subcritical AlN(<2 nm)/GaN structure can induce 2DEG $\sim 1\times10^{13}\,\mathrm{cm}^{-2}$ and can be used for E/D mode HEMTs. As the interface roughness scattering is inherently low[11] in thin-barrier GaN HEMTs, the work presented here can facilitate subcritical barrier HEMTs. Most importantly, the energy band diagram in Fig. 3(b) shows the surprising consequence of polarization: by controlling the effective Q_{it} (for example by compensation doping or by varying the polarization through the composition), V_p can be made to increase, remain independent, or decrease with t_{ox}. Even without the ALD layer, if the top heterointerface satisfies $Q_{it} = Q_{\pi(GaN)}$ using either GaN caps or InAlN cap that is *polarization matched* to GaN (Ref. 20) will render V_p *independent* of the cap layer thicknesses. Though the precise origin of the charges at the heterointerface and the corresponding behavior for the N-polar face remains to be clarified, the strong correlation with the polarization is expected to further our understanding of ALD/III-Nitride interfaces with useful consequences for high-performance devices.

[1] M. A. Khan, X. Hu, G. Simin, A. Lunev, J. Yang, R. Gaska, and M. S. Shur, IEEE Electron Device Lett. **21**, 63 (2000).
[2] J. R. Shealy, T. R. Prunty, E. M. Chumbes, and B. K. Ridley, J. Cryst. Growth. **250**, 7 (2003).
[3] C. Liu, E. F. Chor, and L. S. Tan, Appl. Phys. Lett. **88**, 173504 (2006).
[4] N. Maeda, M. Hiroki, N. Watanabe, Y. Oda, H. Yokoyama, T. Yagi, T. Makimoto, T. Enoki, and T. Kobayashi, Jpn. J. Appl. Phys. **46**, 547 (2007).
[5] B. M. Green, K. K. Chu, E. M. Chumbes, J. A. Smart, J. R. Shealy, and L. F. Eastman, IEEE Electron Device Lett. **21**, 268 (2000).
[6] P. D. Ye, B. Yang, K. K. Ng, J. Bude, G. D. Wilk, S. Halder, and J. C. M. Hwang, Appl. Phys. Lett. **86**, 063501 (2005).
[7] D. H. Kim, V. Kumar, G. Chen, A. M. Wowchak, A. Osinsky, and I. Adesida, Electron. Lett. **43**, 129 (2007).
[8] N. V. Nguyen, O. A. Kirillov, W. Jiang, W. Wang, J. S. Suehle, P. D. Ye, Y. Xuan, N. Goel, K. W. Choi, W. Tsai, and S. Sayan, Appl. Phys. Lett. **93**, 082105 (2008).
[9] H. Xing, D. Deen, Y. Cao, T. Zimmerman, P. Fay, and D. Jena, ECS Trans. **11** 233 (2007).
[10] M. Esposto, S. Krishnamoorthy, D. Nath, S. Bajaj, T. Hung, and S. Rajan, Appl. Phys. Lett. **99**, 133503 (2011).
[11] Y. Cao and D. Jena, Appl. Phys. Lett. **90**, 182112 (2007).
[12] N. Onojima, M. Higashiwaki, J. Suda, T. Kimoto, T. Mimura, and T. Matsui, J. Appl. Phys. **101**, 043703 (2007).
[13] D. Jena, Ph.D. thesis, UCSB, 2003.
[14] I. H. Tan, G. L. Snider, L. D. Chang, and E. L. Hu, J. Appl. Phys. **68**, 4071 (1990).
[15] C. G. Van de Walle and J. Neugebauer, Nature **423** 626 (2003).
[16] M. L. Huang, Y. C. Chang, C. H. Chang, T. D. Lin, J. Kwo, T. B. Wu, and M. Hong, Appl. Phys. Lett. **89**, 012903 (2006).
[17] S. M. Sze, *Physics of Semiconductor Devices*, 2nd ed. (Wiley, New York, 1981), Chap. 9.
[18] T. Mattila and R. M. Nieminen, Phys. Rev B. **54**, 16676 (1996).
[19] T. Zimmermann, Y. Cao, G. Li, G. Snider, D. Jena, and H. Xing, Phys. Status Solidi A **208**, 1 (2011).
[20] D. Jena, J. Simon, A. Wang, Y. Cao, K. Goodman, J. Verma, S. Ganguly, G. Li, K. Karda, V. Potasenko, C. Lian, T. Kosel, P. Fay, and H. Xing, Phys. Status Solidi A **208**, 1 (2011).

Downloaded 09 Nov 2011 to 129.74.250.206. Redistribution subject to AIP license or copyright; see http://apl.aip.org/about/rights_and_permissions